

# Monopole scaling dimension using Monte Carlo

Nikhil Karthik<sup>1,\*</sup>

<sup>1</sup>*Physics Department, Brookhaven National Laboratory, Upton, New York 11973-5000, USA*

## Abstract

We present a viable Monte Carlo determination of the scaling dimensions  $\Delta_Q$  of flux  $Q$  Abelian monopoles through finite-size scaling analysis of the free energy to introduce the background field of classical Dirac monopole-antimonopole pair at critical points of three-dimensional lattice theories. We validate the method in free fermion theory, and by verifying the particle-vortex duality between the monopole scaling dimension at the inverse-XY fixed point and the charge scaling dimension at the XY fixed point. At the  $O(2)$  Wilson-Fisher fixed point, we determine the critical exponents  $\Delta_1 = 0.13(2)$ ,  $\Delta_2 = 0.29(1)$  and  $\Delta_3 = 0.47(2)$ , which we find to be proportional to the finite-size critical spectrum of monopoles on square torus.

arXiv:1808.08970v1 [cond-mat.str-el] 27 Aug 2018

## INTRODUCTION

Classification of all possible relevant operator deformation of critical points is central to understanding critical phenomena, and the field theories which either have their continuum limits at the critical point or flow to the fixed point in the infra-red limit [1]. This involves a computation of scaling dimension of operators at the fixed point. In three dimensions, in addition to the usual local operators which are analytic functions of the field or spin variables in the underlying theory, there are also the disorder operators whose action is to introduce non-trivial winding of the the field or spin variables about the insertion point [2, 3]. In the case of theories with  $U(1)$  symmetry, these are the magnetic monopole operators which introduce  $2\pi Q$  total magnetic flux on spheres enclosing them, and their scaling dimensions  $\Delta_Q$  are a new set of critical exponents.

The relevance of monopole terms in the renormalization group flow could drive quantum field theories to different long distance behaviors, a well known example being the Abelian non-compact and compact QED<sub>3</sub> [4], coupled to small number of massless fermion flavors [5, 6]. In addition to serving as a possible scale-inducing deformation that can be added to a fixed point, the monopoles are one of the actors in the three dimensional particle-vortex dualities in various forms (e.g., [7–11]). These dualities map particles charged under  $U(1)$  of one theory to monopoles of another theory, with the two theories in many cases being tuned to their critical points. The most basic three-dimensional duality is the mathematical correspondence between the Villain form of the XY model at zero electric charge and the gauged XY model at zero temperature but non-zero electric charge [7]. However, many recent particle-vortex dualities are well motivated but nevertheless conjectural (e.g., [8, 9]). Thus, it is imperative that one should be able to compute the critical exponents of monopole operators using standard Monte Carlo methods, to go hand in hand with such recent theoretical developments and also to complement the advancements in bootstrap methodology in finding scaling dimensions [12].

The monopole operators are non-local in terms of the fundamental fields, but behave as local operators [3]. This follows from the state-operator correspondence, in which by construction, the monopole operators are the local primary operators at the origin to which the ground states of a CFT in  $S^2 \times \mathbb{R}$  with net fluxes  $2\pi Q$  over  $S^2$ , are mapped onto [13, 14]. Denoting such a primary monopole operator as  $M_Q(x)$ , its scaling dimension  $\Delta_Q$  at a critical point is determined from its power-law behavior:

$$\langle M_Q(x)M_{-Q}(y) \rangle \propto \frac{1}{|x-y|^{2\Delta_Q}}. \quad (1)$$

In spite of the simplicity of the definition, the actual construction of a monopole operator itself is subtle in  $\mathbb{R}^3$ , making them notoriously difficult to study using the standard Monte Carlo methods [14]. In most cases, the ab initio understanding of monopole operators proceed on a case by case basis, wherein one maps the monopole operator to trivial local operators in a different theory related by an established duality or in the same universality class [15–17].

The motivation for the current work is to use a Monte Carlo method for finding  $\Delta_Q$ , that generalizes to various systems without appealing to properties special to any lattice model, and demonstrate that it works. We do so by coupling the static background  $U(1)$  field from a monopole and antimonopole separated by a non-zero distance, to the conserved currents of critical lattice theories and we measure the free energy required to do so. This technique was first introduced in [2] for the case of  $CP^\infty$  model where the partition function can be exactly computed, and now routinely used in analytic perturbative computations of  $\Delta_Q$  using the state-operator correspondence [2, 5, 6, 13, 14, 18]. From the asymptotic scaling of this free energy with the distance between the monopole and antimonopole, which is kept proportional to the lattice size itself, we determine the monopole scaling dimension. The underlying assumption is that the introduction of a flux  $Q$  Dirac monopole background field leads to dominant contributions from the same configurations that would contribute to the constrained path integral resulting from the insertion of the scaling operator  $M_Q$ , not just in the limit of infinite number of species,  $N$ , of spins or matter fields but for any number  $N$ .

## METHOD

We consider simple fermion and spin systems with  $U(1)$  global symmetry in  $L^3$  periodic lattice. The  $U(1)$  symmetry can be gauged by coupling the spins to dynamical gauge fields  $a_\mu(\mathbf{x})$  which are defined on the links connecting the lattice site  $\mathbf{x}$  to  $\mathbf{x} + \hat{\mu}$ . In addition to the dynamical gauge fields, one can couple the conserved currents of the systems to external background fields  $\mathcal{A}$  in order to construct  $\mathcal{A}$  dependent partition function and effective action,  $Z(\mathcal{A})$  and  $F(\mathcal{A}) = -\log Z(\mathcal{A})$  respectively. In the present work, we set  $\mathcal{A}$  to be a superposition of gauge fields from a monopole at  $\mathbf{r}_0$  and an antimonopole at  $\mathbf{r}'_0$ , which are separated by a distance  $r = |\mathbf{r}_0 - \mathbf{r}'_0|$ , and compute the response of the system to change in  $r$ . That is, the superposed field  $\mathcal{A}^{Q\bar{Q}}(\mathbf{r}; r) = \mathbf{A}^Q(\mathbf{r}; \mathbf{r}_0) - \mathbf{A}^Q(\mathbf{r}; \mathbf{r}'_0)$ , where  $\mathbf{A}^Q(\mathbf{r}; \mathbf{r}_0)$  is the classical, scale-covariant field at a point  $\mathbf{r} = (x, y, z)$  from a Dirac monopole of magnetic charge  $Q \in \mathbb{Z}$  at

$\mathbf{r}_0 = (x_0, y_0, z_0)$  (c.f., [19]) :

$$\mathbf{A}^Q(\mathbf{r}; \mathbf{r}_0) = \frac{Q}{2} \frac{(\mathbf{r} - \mathbf{r}_0) \times \hat{\mathbf{z}}}{|\mathbf{r} - \mathbf{r}_0|(|\mathbf{r} - \mathbf{r}_0| - (z - z_0))}. \quad (2)$$

Instead of naively discretizing the continuum solution on the lattice, we compute the gauge transporters  $\tilde{\mathcal{A}}_\mu^{Q\bar{Q}}(\mathbf{r}; r) = \int_{\mathbf{r}}^{\mathbf{r}+\hat{\mu}} dx_\mu \mathcal{A}_\mu^{Q\bar{Q}}(\mathbf{x}; r)$  exactly, and couple it to the conserved current of the models. On the lattice, we separate  $Q$  and  $\bar{Q}$  by  $\mathbf{r}_0 - \mathbf{r}'_0 = r\hat{\mathbf{z}}$ , such that the center of mass of the  $Q\bar{Q}$ -pair is at the center of the lattice. For this choice,  $r$  is the length of the Dirac string that runs between  $Q$  and  $\bar{Q}$ . Since the lattice is periodic, we take  $\mathbf{A}^Q(\mathbf{x})$  to be (2) if  $x_\mu \leq L$  and force periodicity otherwise. Any jump in  $\mathbf{A}^Q(\mathbf{x})$  itself at  $x_\mu = L$  is proportional to  $1/L$ , and any contribution of such a jump to the effective action will be suppressed further by a surface to volume factor in the thermodynamic limit.

The monopole-antimonopole correlator in the background field method is simply

$$G(r) \equiv \frac{Z(\tilde{\mathcal{A}}^{Q\bar{Q}}(r))}{Z(0)}. \quad (3)$$

One can compute such a difference in free energies with and without the background field through Monte Carlo simulation by introducing auxiliary variables in the action [20]. Let  $\zeta \in [0, Q]$  be such an auxiliary variable, then

$$F(\tilde{\mathcal{A}}^{Q\bar{Q}}(r)) - F(0) = \int_0^Q d\zeta W(\zeta); \quad W(\zeta; r) \equiv \frac{\partial}{\partial \zeta} F(\zeta \tilde{\mathcal{A}}^{1\bar{1}}). \quad (4)$$

The quantity  $W$  is a measurement that can be made in Monte Carlo simulation of  $Z(\zeta \tilde{\mathcal{A}}^{1\bar{1}})$  theory. Henceforth, we refer to the above difference in free energies simply as  $F_Q(r)$ .

We assume that the monopole-antimonopole correlator at the critical point of lattice theories is a scaling function,  $G(r, L, \xi_L) \sim r^{-2\Delta_Q} g\left(\frac{r}{\xi_L}, \frac{r}{L}\right)$ , where  $\xi_L$  is the finite correlation length in the finite system which we will grow linearly with  $L$  at the critical point. There could be corrections from finite size scaling from subleading  $L^{-\omega}$  terms. A finite-size scaling method to determine the exponents  $\Delta_Q$  is to consider the correlation functions at  $r = \rho L$  for a fixed fraction  $\rho$  in different lattice sizes [21]. In such a case,  $G(\rho L, L, \xi_L) \sim L^{-2\Delta_Q} (1 + O(L^{-\omega}))$ . Therefore, we look for the following finite size behavior of free energy with a leading logarithmic term

$$F_Q(\rho L) = f_0(\rho, Q) + 2\Delta_Q \log(L) + \frac{f_1(\rho, Q)}{L^\omega}, \quad (5)$$

in order to extract  $\Delta_Q$ . The value of  $\omega$  for local operators is known in 3d XY and Ising models to be close to 0.8 [22–24]. Due to our lack of knowledge about such scaling-violation exponent for background insertions, we simply use an analytic  $\omega = 1$  which empirically accounts for any

corrections to scaling in the volumes we study. Throughout this paper, we set  $\rho = r/L = 1/4$  for finite-size scaling studies.

## SYSTEMS

To serve as a sanity check, we study the partition function  $Z_F(\mathcal{A})$  for a single two-component free Dirac fermion coupled to the external field  $\mathcal{A}^{Q\bar{Q}}$ . We use the two-component Wilson-Dirac fermion for this purpose, in which case,  $Z_F = \det(\mathcal{D}_W(\mathcal{A}))$  with  $\mathcal{D}_W$  being the Wilson-Dirac operator. Then, we study the chargeless limit and the zero temperature limit of the lattice superconductor model with the action [25]

$$S = -\beta \sum_x \sum_{\mu=1}^3 \cos\left(\nabla_\mu \theta(x) + e a_\mu(x) + \tilde{\mathcal{A}}_\mu^{Q\bar{Q}}(x)\right) + \frac{1}{2} \sum_x \sum_{\mu>\nu=1}^3 (\nabla_\mu a_\nu(x) - \nabla_\nu a_\mu(x))^2, \quad (6)$$

where  $\nabla_\mu f(x) = f(x + \hat{\mu}) - f(x)$ . The first  $e = 0$  case is the XY model, whose critical point at  $\beta_c = 0.4541652$  lies in the  $O(2)$  universality class [22, 26]. The second  $\beta \rightarrow \infty$  limit corresponds to the frozen superconductor (FZS) model whose critical point [25, 27] at  $e_c^2 = 13.148997$  is in the inverse-XY universality class [25]. In the FZS limit, the argument of cosine is forced to take the values  $2\pi n_\mu$  for integer valued  $n_\mu$  [27]. The FZS action becomes

$$S = \frac{2\pi^2}{e^2} \sum_x \sum_{\mu>\nu=1}^3 \left( \nabla_\mu n_\nu(x) - \nabla_\nu n_\mu(x) - \frac{\tilde{\mathcal{F}}_{\mu\nu}^{Q\bar{Q}}(x)}{2\pi} \right)^2, \quad (7)$$

with  $\tilde{\mathcal{F}}_{\mu\nu}^{Q\bar{Q}}(x) = \nabla_\mu \tilde{\mathcal{A}}_\nu^{Q\bar{Q}}(x) - \nabla_\nu \tilde{\mathcal{A}}_\mu^{Q\bar{Q}}(x)$ . An exact particle-vortex duality mapping between the XY model and FZS model was worked out by Peskin [7]. In this duality, the charge- $Q$  operators  $e^{iQ\theta(x)}$  maps onto the monopole operators  $M_Q(x)$  in the FZS model. The critical exponents for the charge- $Q$  operators at XY fixed point are well known [21, 28].

## MONOPOLE CRITICAL EXPONENTS

For the finite-size scaling study, we used periodic  $L^3$  lattices for  $L = 12, 16, 20, 24, 28, 32$  and 36. For each fixed values of  $L$  and  $Q$ , the different  $\zeta$  corresponds to independent Monte Carlo simulations. We used 48 different values of  $\zeta$  from 0 to 3 for each  $L^3$  lattice in order to study  $Q = 1, 2, 3$ . We simulated the XY model at the critical point  $\beta_c$  using Hybrid Monte Carlo (HMC) global updates [29]. We made about  $5.10^6$  measurements in all our lattice sizes. For the FZS model, we used single-hit Metropolis algorithm and made  $10^8$  such updates. Error

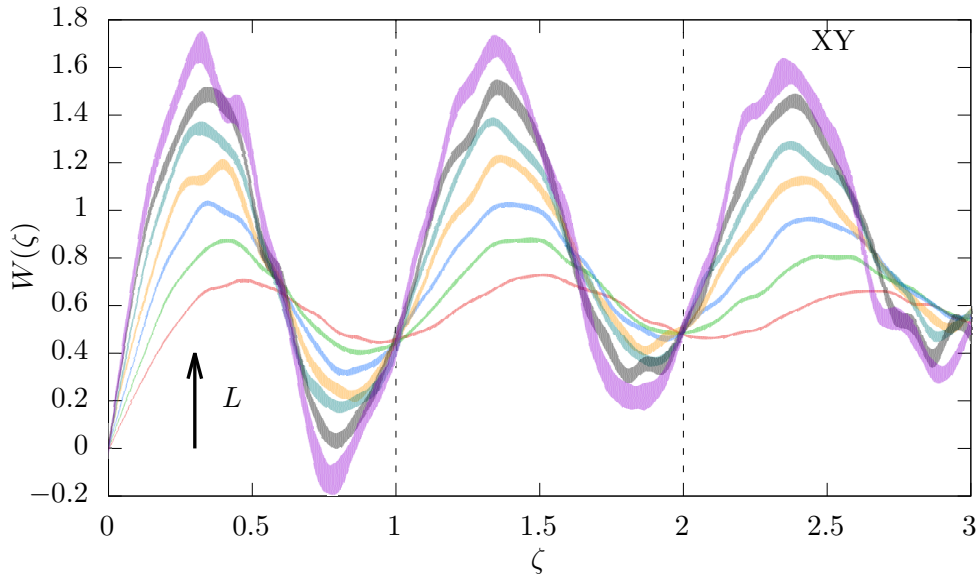


FIG. 1. The function  $W(\zeta)$  is shown in the range 0 to 3 for monopole-antimonopole separation  $r = L/4$  in the critical XY model. The different colored curves are the interpolation curves of  $W(\zeta)$  from different  $L$ . Along the direction of the arrow,  $L = 12, 16, 20, 24, 28, 32$  and  $36$ .

estimates were made using block Jack-knife to account for autocorrelations. For the free Wilson-Dirac fermion, we evaluated  $W(\zeta) = -\text{tr} \left( \mathbb{D}_W^{-1} \mathbb{D}'_W \right)$  stochastically using  $10^4$  random vectors. We also tuned the Wilson mass on  $A^{\text{I}\bar{\text{I}}}$  background so that the lattice fermion is massless [30].

In Figure 1, we show  $W(\zeta; r)$  as a function of  $\zeta$  for the critical XY model. In order to obtain the curves, we interpolated the equally spaced Monte-Carlo data points for  $W(\zeta; r)$  using cubic spline. The different curves correspond to different  $L$  at fixed  $\rho = 1/4$ . In order to obtain the free energy for  $Q$ -monopole, we integrate the splines from 0 up to  $Q$ . We obtain similar such curves for the free fermion as well as the critical FZS model. For all such cases, we observe distinct oscillations in  $W(\zeta; r)$  of period  $\mathcal{O}(1)$ , and the curves corresponding to fixed  $\rho$  approximately intersect each other close to integer values of  $\zeta$ . Due to the charge conjugation symmetry,  $W(\zeta; r)$  is odd in  $\zeta$ , and in our numerical simulations we do find  $W(0; r) = 0$  is satisfied well within error bars, serving as a check. At present, we lack a theoretical understanding of such curves which could help extrapolate the results to larger  $Q$ .

In Figure 2, we show the behavior of free energy  $F_Q(r)$  at fixed  $\rho = 1/4$  as a function of  $\log(L)$ . The three panels from top to bottom correspond to free Wilson-Fermion, critical FZS and critical XY models respectively. The symbols in the plots are the actual Monte Carlo data. The most important observation in this paper is the clear presence of  $\log(L)$  behavior in the background field method and also the onset on this  $\log(L)$  behavior for computationally

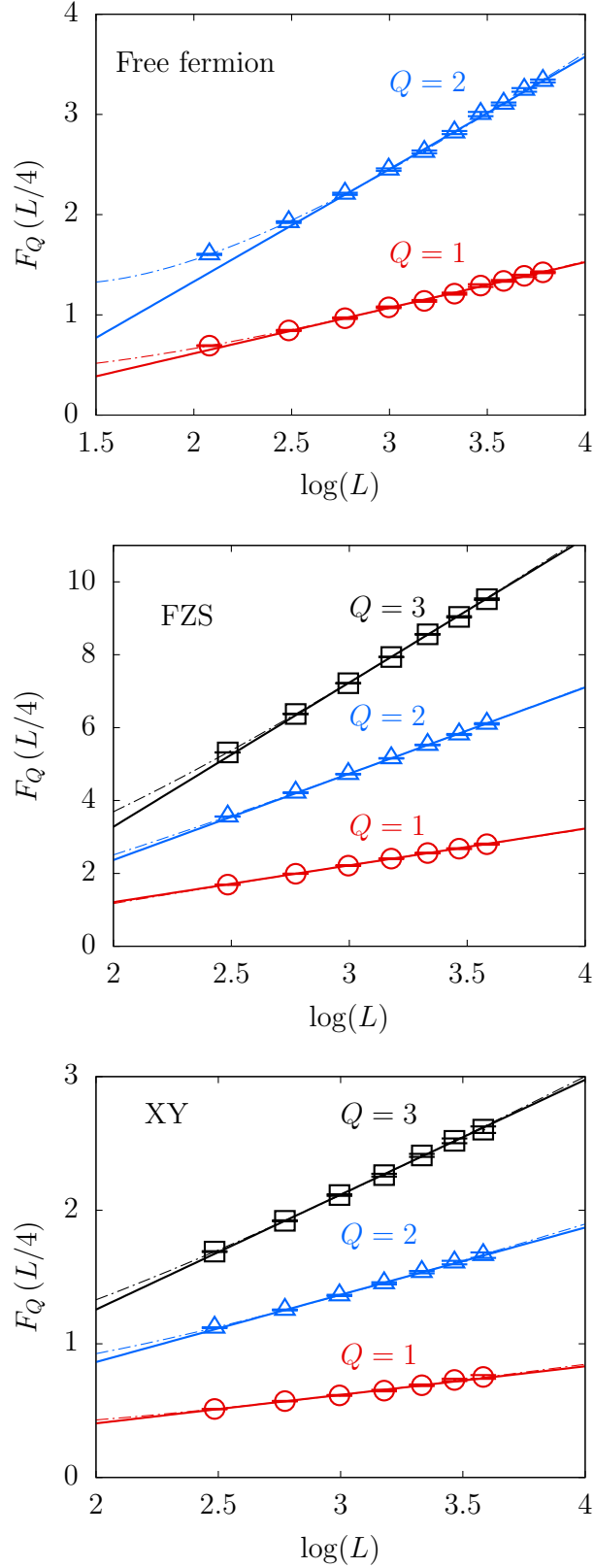


FIG. 2. The free energy of monopole-antimonopole background field insertion is shown as a function of  $\log(L)$  for fixed  $\rho = r/L = 1/4$ . The top panel is for free Wilson-Dirac fermion, the middle panel for the critical frozen superconductor model and the bottom panel for the critical XY model. The curves are fits to the data.

Model	$Q$	$\Delta_Q$		Expectation
Free fermion	1	0.227(4)	0.253(8)	0.265 (e)
	2	0.561(8)	0.66(1)	0.673 (e)
FZS	1	0.51(1)	0.48(2)	0.516(3) (d)
	2	1.18(1)	1.23(2)	1.238(5) (d)
	3	1.97(1)	2.15(4)	2.116(6) (d)
XY	1	0.107(4)	0.13(2)	0.065 (a)
	2	0.252(3)	0.29(1)	0.159 (a)
	3	0.429(5)	0.47(2)	0.272 (a)

TABLE I. Table of estimated scaling dimensions for free Wilson fermion, critical FZS model and critical XY model. The third and the fourth columns tabulate the fit values of  $\Delta_Q$  with and without a  $1/L$  scaling correction term respectively. The fifth column is the expected values; the entries marked (e) are exact results, those marked (d) are inferred from particle-vortex duality, while those marked (a) are expectations based on large- $N$  calculations.

accessible values of  $L$ . The curves are our  $\log(L)$  fits to the data; the solid curve is the straight line fit including just a  $\log(L)$  term using data from  $L > 12$  lattices, while the dashed curves include any  $1/L$  corrections to the free energy in addition to the dominant  $\log(L)$  term. In all the cases, the  $\chi^2/\text{DOF} < 2$  for the fits.

In the case of free continuum fermion, the values of  $\Delta_Q$  are known exactly by computations of the Casimir energy of free fermions on  $S^2$  with constant flux over it [3, 5]. These values for free fermions are tabulated in Table I along with the values of  $\Delta_Q$  extracted from fits to the data. There is about 15% systematic dependence on the kind of fit. With a  $1/L$  correction term included in the fit, the free energy from all  $L$  are well described by the fit (Figure 2), and the corresponding fit values of  $\Delta_Q$  agree quite well with the analytical results from free continuum Dirac fermion. While serving as a check on the method, it is also a fascinating check on the universality of the nontrivial monopole critical exponent itself as it is determined using a lattice fermion which only lies in the same universality class as the free continuum fermion.

The middle panel of Figure 2 shows the result for the critical FZS model. From the corresponding entries in Table I, an excellent agreement with the charge scaling dimensions in  $O(2)$  fixed point is seen. This is expected from the exact particle-vortex duality [7]. However, it is an important check that the background field method leads to the same critical exponents as those of the primary monopole operators that enter the duality, thereby supporting our assumption.



Having demonstrated the method in two different cases where the values of  $\Delta_Q$  are available from other means, we apply the method to  $O(2)$  fixed point. There are no dynamical gauge fields in this case, however one can still insert an external monopole operator that creates  $U(1)$  vortices in  $\theta$  fields [5]. The  $\log(L)$  dependence of free energy data and the fits are shown in the bottom panel of Figure 2, and we have tabulated the fit values of  $\Delta_Q$  in Table I. There is about 10% systematic dependence of  $\Delta_Q$  on the type of fit. Next to our estimates of  $\Delta_Q$ , we also tabulate the expected values from  $1/N$  extrapolation of  $\Delta_Q$  calculated in  $O(2N)$  fixed points for large- $N$  [5]. The estimated values are about twice the extrapolated values, perhaps indicating non-negligible nonperturbative corrections to  $\Delta_Q$  for smaller  $N$ . However, the conclusion that monopole operators with  $Q = 1, 2, 3$  are relevant ( $\Delta_Q < 3$ ) at  $O(2)$  fixed point still remains true.

## FINITE-SIZE SPECTRUM

Recently, the universal features in the finite-size critical spectrum of operators have been of interest [31–33]. Here, we provide a computation of critical spectrum of Dirac monopole at the  $O(2)$  fixed point of XY model. For this, we use  $L^2 \times 4L$  lattices as an approximation for  $T^2 \times \mathbb{R}$ , and compute the torus finite-size spectrum  $E_Q L$  from the slope of a linear increase in  $F_Q(r)$  with  $r/L$ , for  $L < r < 2L$  in the thermodynamic limit  $L \rightarrow \infty$ . The free energy corresponding to such an ‘exponential decay’ of the monopole-antimonopole correlator is shown for XY model in the top panel of Figure 3 on  $16^2 \times 64$  lattice for  $r/L > 1$ . In the bottom panel, we show the thermodynamic limit of the extracted  $E_Q L$  using quadratic polynomials in  $1/L$ . The existence of the thermodynamic limit of  $E_Q L$  is noteworthy and indicates that the extracted spectrum indeed is that of a critical theory. We find  $\sqrt{4\pi}\Delta_Q/(E_Q L)$  to be 0.29(5), 0.37(2), 0.33(2) for  $Q = 1, 2, 3$  respectively, indicating a near proportionality between  $\Delta_Q$  and  $E_Q$  starting from small values of  $Q$ . Such a ratio for the charge- $Q$  operators,  $\exp(iQ\theta)$ , in the XY model was shown to be about 1 even for small  $Q$  [21, 34].

## DISCUSSION

We demonstrated the effectiveness of a rather straight-forward numerical implementation of the background field method in determining the monopole scaling dimensions, as applied to both fermionic and bosonic critical lattice theories. We chose simple theories here in order to test the feasibility of the approach. The successful application of the method in demonstrating

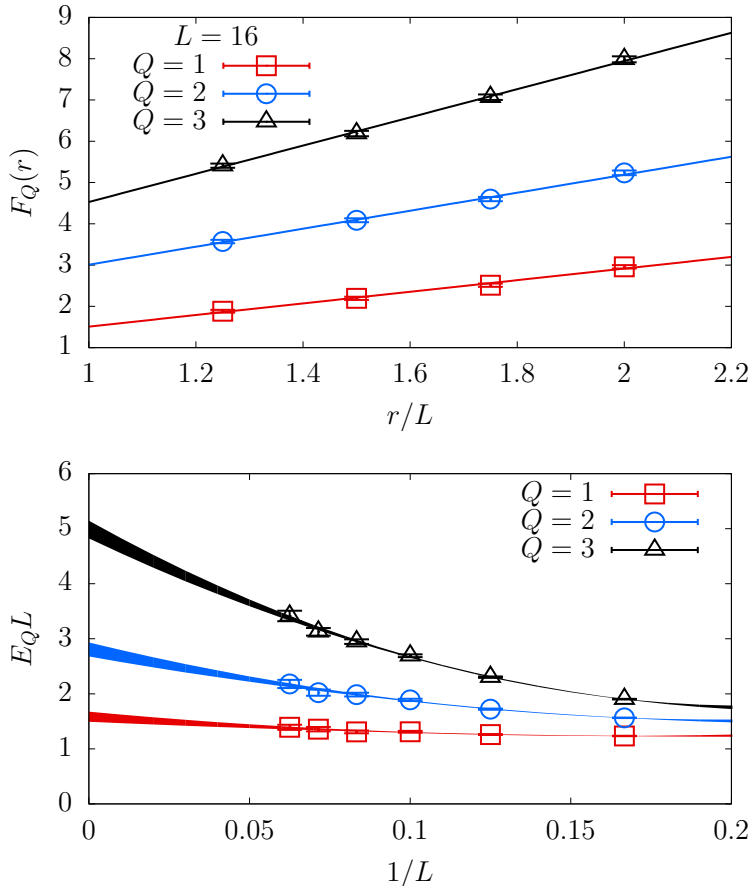


FIG. 3. Spectrum  $E_Q$  of monopoles on torus as determined on  $L^2 \times 4L$  lattice is shown for the critical XY model. The top panel shows the linear dependence of free energy with the monopole-antimonopole separation  $r$ , for  $r > L$ . The bottom panel shows the extrapolation of  $E_Q L$  to the thermodynamic limit.

an exact particle-vortex duality [7] provides ample motivation to apply the method to recently conjectured particle-vortex dualities. It would also be interesting to repeat this computation for the monopole scaling dimension in the infra-red fixed point of non-compact QED<sub>3</sub> with  $N$  flavors of massless Dirac fermions to determine the critical  $N$  where monopoles become irrelevant, and check if it matches with the critical  $N$  for compact QED<sub>3</sub>. The near proportionality of  $\Delta_Q$  with the torus spectrum  $E_Q$  also suggests there could be universality in the monopole finite-size spectrum similar to the findings in [31–33].

I would like to thank R. Narayanan for extensive discussions and critical reading of the manuscript. I thank D. Banerjee, S. Chandrasekharan, R. Dandekar, S. Minwalla, R. Pisarski, and S. Pufu for useful discussions. The computations presented in the paper were carried out using the BC cluster at Fermilab under a USQCD type-C project. I thank the Nuclear Theory Group at BNL for supporting my research. I acknowledge support by the U.S. Department of

Energy under contract No. de-sc0012704.

---

\* nkarthik@bnl.gov

- [1] J. B. Kogut, Rev. Mod. Phys. **51**, 659 (1979).
- [2] G. Murthy and S. Sachdev, Nucl. Phys. **B344**, 557 (1990).
- [3] V. Borokhov, A. Kapustin, and X.-k. Wu, JHEP **11**, 049 (2002), arXiv:hep-th/0206054 [hep-th].
- [4] A. M. Polyakov, Phys. Lett. **59B**, 82 (1975).
- [5] S. S. Pufu and S. Sachdev, JHEP **09**, 127 (2013), arXiv:1303.3006 [hep-th].
- [6] S. S. Pufu, Phys. Rev. **D89**, 065016 (2014), arXiv:1303.6125 [hep-th].
- [7] M. E. Peskin, Annals Phys. **113**, 122 (1978).
- [8] N. Seiberg, T. Senthil, C. Wang, and E. Witten, Annals Phys. **374**, 395 (2016), arXiv:1606.01989 [hep-th].
- [9] A. Karch and D. Tong, Phys. Rev. **X6**, 031043 (2016), arXiv:1606.01893 [hep-th].
- [10] M. A. Metlitski and A. Vishwanath, Phys. Rev. **B93**, 245151 (2016), arXiv:1505.05142 [cond-mat.str-el].
- [11] D. F. Mross, J. Alicea, and O. I. Motrunich, Phys. Rev. Lett. **117**, 016802 (2016), arXiv:1510.08455 [cond-mat.str-el].
- [12] D. Poland and D. Simmons-Duffin, Nature Phys. **12**, 535 (2016).
- [13] M. A. Metlitski, M. Hermele, T. Senthil, and M. P. A. Fisher, Phys. Rev. **B78**, 214418 (2008), arXiv:0809.2816 [cond-mat.str-el].
- [14] E. Dyer, M. Mezei, and S. S. Pufu, (2013), arXiv:1309.1160 [hep-th].
- [15] M. S. Block, R. G. Melko, and R. K. Kaul, Phys. Rev. Lett. **111**, 137202 (2013), arXiv:1307.0519 [cond-mat.str-el].
- [16] G. J. Sreejith and S. Powell, Phys. Rev. **B92**, 184413 (2015), arXiv:1504.02278 [cond-mat.stat-mech].
- [17] S. Pujari, K. Damle, and F. Alet, Phys. Rev. Lett. **111**, 087203 (2013).
- [18] E. Dyer, M. Mezei, S. S. Pufu, and S. Sachdev, JHEP **06**, 037 (2015), [Erratum: JHEP03,111(2016)], arXiv:1504.00368 [hep-th].
- [19] Y. M. Shnir, *Magnetic Monopoles*, Text and Monographs in Physics (Springer, Berlin/Heidelberg, 2005).

- [20] K. Kajantie, M. Laine, T. Neuhaus, J. Peisa, A. Rajantie, and K. Rummukainen, Nucl. Phys. **B546**, 351 (1999), arXiv:hep-ph/9809334 [hep-ph].
- [21] D. Banerjee, S. Chandrasekharan, and D. Orlando, Phys. Rev. Lett. **120**, 061603 (2018), arXiv:1707.00711 [hep-lat].
- [22] M. Hasenbusch and T. Torok, J. Phys. **A32**, 6361 (1999), arXiv:cond-mat/9904408 [cond-mat].
- [23] M. Campostrini, M. Hasenbusch, A. Pelissetto, and E. Vicari, Phys. Rev. **B74**, 144506 (2006), arXiv:cond-mat/0605083 [cond-mat].
- [24] M. Hasenbusch, J. Phys. **A34**, 8221 (2001), arXiv:cond-mat/0010463 [cond-mat].
- [25] C. Dasgupta and B. I. Halperin, Phys. Rev. Lett. **47**, 1556 (1981).
- [26] M. Campostrini, M. Hasenbusch, A. Pelissetto, P. Rossi, and E. Vicari, Phys. Rev. **B63**, 214503 (2001), arXiv:cond-mat/0010360 [cond-mat].
- [27] T. Neuhaus, A. Rajantie, and K. Rummukainen, Phys. Rev. **B67**, 014525 (2003), arXiv:cond-mat/0205523 [cond-mat].
- [28] M. Hasenbusch and E. Vicari, Phys. Rev. B **84**, 125136 (2011).
- [29] S. Duane, A. Kennedy, B. Pendleton, and D. Roweth, Phys.Lett. **B195**, 216 (1987).
- [30] N. Karthik and R. Narayanan, Phys. Rev. **D93**, 045020 (2016), arXiv:1512.02993 [hep-lat].
- [31] A. Thomson and S. Sachdev, Phys. Rev. **B95**, 205128 (2017), arXiv:1607.05279 [cond-mat.str-el].
- [32] M. Schuler, S. Whitsitt, L.-P. Henry, S. Sachdev, and A. M. Luchli, Phys. Rev. Lett. **117**, 210401 (2016), arXiv:1603.03042 [cond-mat.str-el].
- [33] S. Whitsitt, M. Schuler, L.-P. Henry, A. M. Luchli, and S. Sachdev, Phys. Rev. **B96**, 035142 (2017), arXiv:1701.03111 [cond-mat.str-el].
- [34] S. Hellerman, D. Orlando, S. Reffert, and M. Watanabe, JHEP **12**, 071 (2015), arXiv:1505.01537 [hep-th].

## Monopole background on the lattice

We use periodic  $L_x \times L_y \times L_z$  lattice; for finite-size scaling studies,  $L_x = L_y = L_z = L$ , while for extracting torus spectrum,  $L_x = L_y = L$  and  $L_z = 4L$ , and we use even values of  $L$ . Let us arbitrarily choose a point on the periodic lattice as the origin which has coordinates as  $(1, 1, 1)$ . With respect to this origin, consider a monopole of magnetic charge  $Q$  at  $\mathbf{r}_0 = (x_0, y_0, z_0)$ . The Dirac monopole background is

$$\mathbf{A}^Q(\mathbf{r}; \mathbf{r}_0) = \frac{Q}{2} \frac{(\mathbf{r} - \mathbf{r}_0) \times \hat{\mathbf{z}}}{|\mathbf{r} - \mathbf{r}_0|(|\mathbf{r} - \mathbf{r}_0| - (z - z_0))}. \quad (8)$$

These field variables are the parallel transporters which live on the links of the lattice. Therefore, the link variables connecting point  $\mathbf{n} = (x, y, z)$  to  $\mathbf{n} + \hat{\mu}$  is

$$\tilde{\mathbf{A}}_\mu^Q(\mathbf{n}; \mathbf{r}_0) = \int_{\mathbf{n}}^{\mathbf{n} + \hat{\mu}} dx_\mu A_\mu^Q(x; \mathbf{r}_0). \quad (9)$$

Doing the above integrals, we get

$$\begin{aligned} \tilde{A}_1^Q(x, y, z; \mathbf{r}_0) &= \frac{Q}{2} \frac{y - y_0}{|y - y_0|} [f_1(x - x_0 + 1, y - y_0, z - z_0) \\ &\quad - f_1(x - x_0, y - y_0, z - z_0)], \\ \tilde{A}_2^Q(x, y, z; \mathbf{r}_0) &= -\frac{Q}{2} \frac{x - x_0}{|x - x_0|} [f_2(x - x_0, y - y_0 + 1, z_0) \\ &\quad - f_2(x_0, y - y_0, z - z_0)], \\ \tilde{A}_3^Q(x, y, z; \mathbf{r}_0) &= 0, \end{aligned} \quad (10)$$

where

$$\begin{aligned} f_1(x, y, z) &= \tan^{-1} \left( \frac{x}{|y|} \right) + \tan^{-1} \left( \frac{xz}{|y| \sqrt{x^2 + y^2 + z^2}} \right), \\ f_2(x, y, z) &= \tan^{-1} \left( \frac{y}{|x|} \right) + \tan^{-1} \left( \frac{yz}{|y| \sqrt{x^2 + y^2 + z^2}} \right). \end{aligned} \quad (11)$$

On a periodic lattice it is not possible to have a single monopole. So, we consider the background field to be the superposition of the fields due to monopole at position  $\mathbf{r}_0$  and an anti-monopole at position  $\mathbf{r}'_0$ , which we place in the dual lattice, in such a way that the pair is almost at the ‘center’ of the periodic lattice with respect to the coordinate system set by the arbitrary choice of the origin:

$$\mathbf{r}_0 = \begin{cases} \left( \frac{L+1}{2}, \frac{L+1}{2}, \frac{L+r+1}{2} \right) & \text{even } r \\ \left( \frac{L+1}{2}, \frac{L+1}{2}, \frac{L+r}{2} \right) & \text{odd } r, \end{cases} \quad \mathbf{r}'_0 = \begin{cases} \left( \frac{L+1}{2}, \frac{L+1}{2}, \frac{L-r+1}{2} \right) & \text{even } r \\ \left( \frac{L+1}{2}, \frac{L+1}{2}, \frac{L-r}{2} \right) & \text{odd } r. \end{cases} \quad (12)$$

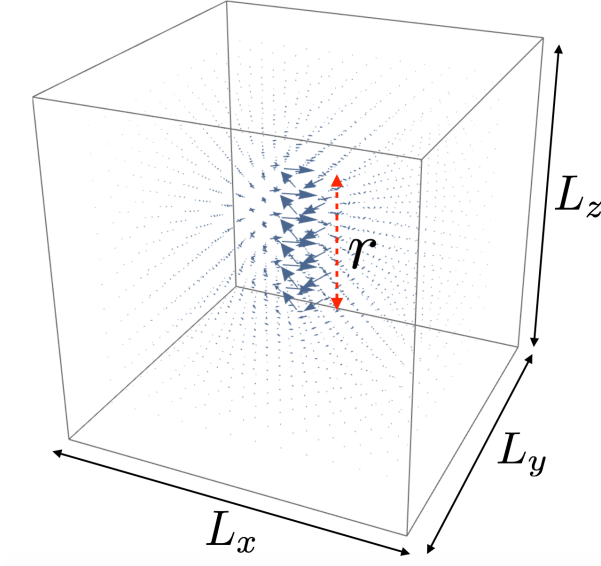


FIG. 4. The background field  $\mathcal{A}^{Q\bar{Q}}$  from monopole-antimonopole pair (the blue arrows) in a periodic  $L_x \times L_y \times L_z$  lattice box. The distance between monopole and antimonopole is  $r$ , and they are separated along the  $z$ -direction.

The superposed field from the monopole-antimonopole pair is

$$\tilde{\mathcal{A}}_\mu^{Q\bar{Q}}(x, y, z; r) = \tilde{A}_\mu^Q(x, y, z; \mathbf{r}_0) - \tilde{A}_\mu^Q(x, y, z; \mathbf{r}'_0), \quad (13)$$

for  $1 \leq x \leq L_x$ ,  $1 \leq y \leq L_y$  and  $1 \leq z \leq L_z$ . For  $x_\mu \rightarrow x_\mu + L_\mu$ , we force periodic boundary conditions on  $\tilde{\mathcal{A}}^{Q\bar{Q}}$ .

### Hybrid Monte Carlo for XY model

We use hybrid Monte Carlo (HMC) [29] global updates to simulate the XY model. Below, we give the HMC force calculation for the general lattice superconductor model with non-zero  $e$ , of which the XY model corresponds to  $e = 0$ . For HMC, we introduce the auxiliary momenta  $\Pi(x)$  conjugate to  $\theta(x)$  and  $\pi_\mu(x)$  conjugate to  $a_\mu(x)$ . For the fictitious Hamiltonian  $\mathcal{H}$ ,

$$\mathcal{H} = \frac{1}{2} \sum_x \Pi^2(x) + \frac{1}{2} \sum_{x,\mu} \pi_\mu^2(x) + S_{XY}(\zeta \mathcal{A}^{1\bar{1}}). \quad (14)$$

where  $S_{XY}$  is the action in Eq. (6) with the replacement  $\mathcal{A}^{Q\bar{Q}} \rightarrow \zeta \mathcal{A}^{1\bar{1}}$  in order to find  $W(\zeta)$ .

The molecular dynamics evolution through Monte Carlo time  $\tau$  is

$$\begin{aligned} \frac{d\Pi(x)}{d\tau} &= -\frac{\partial S}{\partial \theta(x)}; & \frac{d\pi_\mu(x)}{d\tau} &= -\frac{\partial S}{\partial a_\mu(x)}, \\ \frac{d\theta(x)}{d\tau} &= \Pi(x); & \frac{da_\mu(x)}{d\tau} &= \pi_\mu(x). \end{aligned} \quad (15)$$

The explicit expressions are

$$\begin{aligned}
\frac{d\Pi(x)}{d\tau} &= \beta \sum_{\mu=1}^3 \left[ \sin \left( \nabla_{\mu}\theta(x) + ea_{\mu}(x) + \zeta \mathcal{A}_{\mu}^{1\bar{1}}(x) \right) \right. \\
&\quad \left. - \sin \left( \nabla_{\mu}\theta(x - \hat{\mu}) + ea_{\mu}(x - \hat{\mu}) + \zeta \mathcal{A}_{\mu}^{1\bar{1}}(x - \hat{\mu}) \right) \right], \\
\frac{d\pi_{\mu}(x)}{d\tau} &= -\frac{1}{2} \sum_{\nu \neq \mu} \left[ a_{\nu}(x + \hat{\mu}) - a_{\mu}(x + \hat{\nu}) - a_{\nu}(x) \right. \\
&\quad \left. + a_{\nu}(x - \hat{\nu}) - a_{\mu}(x - \hat{\nu}) - a_{\nu}(x - \hat{\nu} + \hat{\mu}) \right] \\
&\quad - e\beta \sin \left( \nabla_{\mu}\theta(x) + ea_{\mu}(x) + \zeta \mathcal{A}_{\mu}(x) \right).
\end{aligned} \tag{16}$$

### Determination of $W(\zeta)$

The definition of  $W$  is

$$W(\zeta; r) \equiv \frac{-1}{Z(\zeta \mathcal{A}^{1\bar{1}})} \frac{\partial Z(\zeta \mathcal{A}^{1\bar{1}})}{\partial \zeta}. \tag{17}$$

The right-hand side can be expressed as an ensemble average of quantities evaluated in the simulation with actions  $S(\zeta \mathcal{A}^{1\bar{1}})$ . Denoting such ensemble averages as  $\langle \dots \rangle_{\zeta}$ , the expression for  $W$  in the XY model is

$$W(\zeta) = \beta \left\langle \sum_x \sum_{\mu=1}^3 A_{\mu}^{1\bar{1}}(x) \sin \left( \nabla_{\mu}\theta(x) + \zeta A_{\mu}^{1\bar{1}}(x) \right) \right\rangle_{\zeta}. \tag{18}$$

For the FZS model,

$$\begin{aligned}
W(\zeta) &= \frac{4\pi^2}{e^2} \sum_x \sum_{\mu > \nu=1}^3 \frac{\tilde{\mathcal{F}}_{\mu\nu}^{1\bar{1}}(x)}{2\pi} (\nabla_{\mu}n_{\nu}(x) - \nabla_{\nu}n_{\mu}(x) \\
&\quad - \zeta \frac{\tilde{\mathcal{F}}_{\mu\nu}^{1\bar{1}}(x)}{2\pi}).
\end{aligned} \tag{19}$$

Now for the case of free Wilson-Dirac fermion. To avoid the trivial zero mode in free field theory, we apply anti-periodic boundary condition in the  $z$ -direction. The Dirac operator is

$$\begin{aligned}
\mathcal{D}_W(x, y) &= (3 - M_W)\delta_{x,y} + \frac{1}{2} \sum_{k=1}^3 \{ (\sigma_k + 1)U_{\mu}(x)\delta_{x+\hat{k},y} \\
&\quad + (1 - \sigma_k)U_{\mu}^*(x - \hat{k})\delta_{x-\hat{k},y} \},
\end{aligned} \tag{20}$$

where  $\sigma_k$  are Pauli matrices,  $U_k(x) = e^{i\zeta \tilde{\mathcal{A}}_k^{1\bar{1}}(x)}$ , and  $M_W$  is the Wilson mass which we tune such that the second smallest eigenvalue of  $\mathcal{D}_W^{\dagger} \mathcal{D}_W$  is minimized as a function of  $M_W$  on  $\mathcal{A}^{1\bar{1}}$  background. Taking the derivative of  $F(\zeta \mathcal{A}^{1\bar{1}}) = -\log \det \mathcal{D}_W$ ,

$$\begin{aligned}
W(\zeta) &= -\frac{1}{\det \mathcal{D}_W} \frac{\partial}{\partial \zeta} \det \mathcal{D}_W, \\
&= -\text{Tr} \left( \mathcal{D}_W^{-1} \frac{\partial \mathcal{D}_W}{\partial \zeta} \right).
\end{aligned} \tag{21}$$

The explicit expression for the derivative is

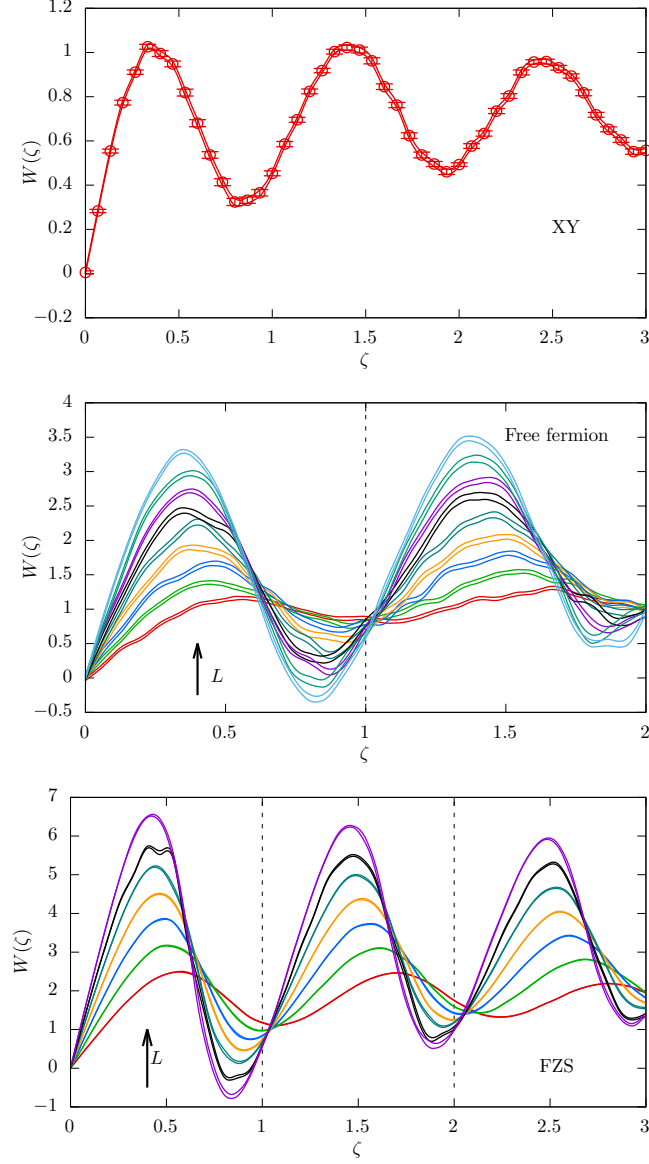


FIG. 5. Top panel shows  $W(\zeta)$  for the critical XY model at  $r/L = 1/4$  on  $L = 20$  lattice. The measurements of  $W(\zeta)$  are the red circles, while the red band is the  $1\text{-}\sigma$  error band from the cubic spline interpolation. The middle panel shows  $W(\zeta)$  for free Wilson-Dirac fermion and the bottom one for the critical FZS model. The different color bands correspond to different  $L$  at fixed  $r/L = 1/4$ . Along the direction of the arrow, the values of  $L$  for free fermion are  $L = 12, 16, 20, 24, 28, 32, 36, 40, 44$  respectively. For the FZS model, it is  $L = 12, 16, 20, 24, 28, 32, 36$  respectively.

$$\begin{aligned}
\frac{\partial}{\partial \zeta} \mathcal{D}_W(x, y) = & \frac{i}{2} \sum_{k=1}^3 \{ (\sigma_k + 1) A_k^{1\bar{1}}(x) U_\mu(x) \delta_{x+\hat{k}, y} \\
& - (1 - \sigma_k) A_k^{1\bar{1}}(x - \hat{k}) U_\mu^*(x - \hat{k}) \delta_{x-\hat{k}, y} \}.
\end{aligned} \tag{22}$$



Using these expressions, we determine the trace stochastically using  $N_v \approx 10^4$  Gaussian random vectors  $R_i$  satisfying  $\overline{R_i^{*a} R_j^b} = \delta_{i,j} \delta_{a,b}$ :

$$W(\zeta) = -\frac{1}{N_v} \sum_{i=1}^{N_v} \left\{ R_i^\dagger \mathcal{D}_W^{-1} \frac{\partial \mathcal{D}_W}{\partial \zeta} R_i \right\}. \quad (23)$$

We used 48 different values of  $\zeta$  from 0 to 3 in the case of XY and FZS models, and up to 2 for free fermion due to the extra computation with the fermion inversion. We interpolated the actual Monte Carlo data for  $W(\zeta)$  using cubic-spline and integrated the spline to get the free energy. In the top panel of Figure 5, we show the data as circles and the cubic spline interpolation of this data as the red, 1- $\sigma$  error band. The middle and bottom panels of Figure 5 show the behavior of  $W(\zeta)$  for free Wilson-Dirac fermion and critical FZS model respectively.